Dalton Transactions

Accepted Manuscript

This article can be cited before page numbers have been issued, to do this please use: M. Lelli, N. Roveri, C. Marzano, J. D. Hoeschele, A. Curci, N. Margiotta, V. Gandin and G. Natile, *Dalton Trans.*, 2016, DOI: 10.1039/C6DT01976E.

This is an *Accepted Manuscript*, which has been through the Royal Society of Chemistry peer review process and has been accepted for publication.

Accepted Manuscripts are published online shortly after acceptance, before technical editing, formatting and proof reading. Using this free service, authors can make their results available to the community, in citable form, before we publish the edited article. We will replace this *Accepted Manuscript* with the edited and formatted *Advance Article* as soon as it is available.

You can find more information about *Accepted Manuscripts* in the Information for Authors.

Please note that technical editing may introduce minor changes to the text and/or graphics, which may alter content. The journal's standard Terms & Conditions and the Ethical guidelines still apply. In no event shall the Royal Society of Chemistry be held responsible for any errors or omissions in this *Accepted Manuscript* or any consequences arising from the use of any information it contains.

ROYAL SOCIETY OF CHEMISTRY

www.rsc.org/dalton

View Article Online
DOI: 10.1039/C6DT01976E

Hydroxyapatite nanocrystals as smart, pH sensitive, delivery system for kiteplatin.

Marco Lelli[a], *Norberto Roveri*[a], *Cristina Marzano*[b], *James D. Hoeschele*[c], *Alessandra Curci*[d], *Nicola Margiotta*[d,*], *Valentina Gandin*[b,*], *Giovanni Natile*[d].

[a]Bioecoactive S.r.l., via San Donato n.5, 40050 Granarolo (Italy);

[b]Dipartimento di Scienze del Farmaco, Università di Padova, Via Marzolo 5, 35131, Padova (Italy);

[c]Department of Chemistry, Eastern Michigan University, 48197 Ypsilanti, MI (USA);

[d]Dipartimento di Chimica, Università degli Studi di Bari Aldo Moro, Via E. Orabona 4, 70125, Bari (Italy).

Abstract

Hydroxyapatite (HA) nanocrystals are important inorganic constituents of biological hard tissues in vertebrates and have been proposed as bone substitute or coating material for prostheses in biomedicine. Hydroxyapatite is also amenable for its capacity to bind to a great variety of biomolecules and therapeutic agents. As drug carriers, apatite nanoparticles have also the advantage of having a pH dependent solubility and low toxicity. Thus HA nanoparticles are negligibly soluble at physiological pH but their dissolution is accelerated at lower pH such as that typically found in the vicinity of tumors. In the present study we have investigated the adsorption on and the release from biomimetic HA nanoparticles of two platinum derivatives of *cis*-1,4-diaminocyclohexane ([PtX_2(*cis*-1,4-DACH)], X_2 = Cl_2 (**1**) or 1,1-cyclobutanedicarboxylate (CBDCA, **2**)). The first of the two compounds proved to be active against colon cancer cells also resistant to oxaliplatin. The release has been investigated as a function of pH to mimic the different physiological environment of healthy tissues and tumors, and the

View Article Online
DOI: 10.1039/C6DT01976E

in vitro cytotoxicity of the releasates from the HA matrices has been assessed against various human cancer cell lines. The results fully confirmed the potential of **1**-loaded HA nanoparticles as bone-specific drug delivery devices.

Keywords: biomimetic hydroxyapatite nanocrystals, kiteplatin, *cis*-1,4-DACH, antitumor platinum drugs, cisplatin.

Introduction

Nanoparticles are promising tools to target tumor cells.[1-2] Nanoparticulate delivery systems offer the opportunity to prolong the circulation in the bloodstream and hence to increase the possibility of accumulation at the tumor sites by taking advantage of the Enhanced Permeability and Retention (EPR) effect, to specifically target cells or tissues of interest via conjugation with ligands specific for cell surface biomolecules, to respond to local stimuli in vivo (such as changes in pH and temperature), and to overcome the cell membrane barrier and avoid the degradation by lysosomes.[3] Ideally, a delivery system consists of: (i) non-toxic starting materials and degradation products, (ii) improved uptake achieved by size in the range of 10-100 nm and large surface area, (iii) colloidal stability of the delivery system (to avoid agglomeration during circulation in vivo), (iv) long clearance times (to permit adequate time for the delivery system to reach target cells), (v) controlled and sustained release of the active agent, and (vi) targetability of the delivery system (to enable delivery of particles to selected cells).[4]

Calcium phosphate is the most important inorganic constituent of biological hard tissues in vertebrates.[5,6] In the form of carbonate-containing hydroxyapatite (HA), calcium phosphate is

View Article Online
DOI: 10.1039/C6DT01976E

present in bone, teeth and cartilaginous tissues. Bones are the most typical calcified tissues in organisms and their shape and size are optimized to achieve best protection and mechanical support for the body. The size of bone crystals, despite variations due to different methods of preparation and analysis of the sample, is generally in the range of nanometers (30–50 nm length, 15–30 nm width, and 2–10 nm thickness).[7,8] It was recently demonstrated that the nanometer size of mineral particles is used in nature to ensure optimum strength and maximum tolerance of flaws.[9,10]

Based on the similarities between synthetic HA and inorganic crystals present in natural bones, synthetic HA has been proposed as bone substitute and/or replacement in biomedicine either in the form of implant material or as agent for surface modification of prostheses to enhance the calcification process of teeth and bones.[6] Research effort has also been devoted to learn more about the chemical process of formation of this mineral in vivo.[11] Several methodologies have been proposed for the synthesis of nanocrystalline hydroxyapatite, the most used are sol–gel synthesis, co-precipitation, mechanochemical synthesis, hydrothermal reaction, and vibro-milling from natural bones.[12-15] Dimensions, morphology, crystallinity and surface properties are the major physico-chemical properties which need to be tailored for optimizing the specific biomedical application of synthetic HA nanocrystals.[16]

Hydroxyapatite is also amenable for its capability to bind a wide variety of biological molecules[17-20] and therapeutic agents,[21,22] thus matching a major challenge for advanced bone substitute biomaterials, that is their functionalization with bioactive molecules.[23-31] Moreover, the adsorption and release properties of the loaded bioactive molecules can be optimized by acting on chemical and structural characteristics of the HA substrate.[28]

View Article Online
DOI: 10.1039/C6DT01976E

As drug carriers, apatite nanoparticles have also the advantage of having lower toxicity than silica nanoparticles, quantum dots, carbon nanotubes, or magnetic particles and to have a greater stability/robustness than organic liposomes. For instance, contrary to liposomes and other micelle-based carriers, which are subject to dissipation below specific critical concentrations (a clear obstacle to their intravenous administration), HA nanoparticles are negligibly soluble in blood and can be used as reliable drug delivery system.[32]

Interestingly, the dissolution of calcium phosphates is accelerated by low pH, such as that typically found in the vicinity of tumors, providing an advantage in the delivery of drugs into malign zones. They are also able to permeate the cell membrane and dissolve affording their ionic constituents (Ca^{2+} and PO_4^{3-}), which are already present in relatively high concentration (1-5 mM) in cells and in the bloodstream. Their dissolution prevents the undesirable accumulation of nanoparticles in cells and tissues, a flaw often encountered with other inorganic and metallic nanoparticle systems. Finally, HA nanoparticles have been recently shown to inhibit colon cancer HCT116 cells by inducing large production of inflammatory cytokines leading to decreased cell proliferation. This effect is correlated with the low crystallinity of the HA powders that results in higher dissolution in the physiological medium and increased calcium uptake in the tumor cells.[33]

Platinum(II) based drugs, such as cisplatin, carboplatin and oxaliplatin (Chart 1) are the first line treatment for many types of malignancies, including testicular, ovarian and lung cancers.[34]A valuable new candidate platinum anticancer drug is [$PtCl_2$(*cis*-1,4-DACH)] (DACH = diaminocyclohexane), also named kiteplatin (**1** in Chart 1), that contains an isomeric form of the oxaliplatin diamine ligand *1R,2R*-DACH. In particular, the interest in this compound stems from its activity against cisplatin (ovarian cancer cells 2008/C13*) and oxaliplatin sensitive and resistant cell lines (colon cancer cells LoVo/LoVo-OXP).[35] Tested *in vivo* in a syngeneic murine solid tumor, the Lewis Lung Carcinoma

View Article Online
DOI: 10.1039/C6DT01976E

(LLC), kitepkatin showed an antitumor effect similar to that of cisplatin and, most importantly, was less toxic than the reference metallo-drug.

In the present study our aim was to assess if the above described characteristics of HA nanoparticles could be exploited to achieve a specific delivery and accumulation of kiteplatin (or its CBDCA derivative) at the acidic tumor sites (where HA nanoparticles dissolve).

Therefore, we have preliminarily investigated the adsorption on and the release from biomimetic HA nanocrystals of kiteplatin and of its 1,1-cyclobutanedicarboxylate derivative [Pt(CBDCA)(*cis*-1,4-DACH)] (**2** in Chart 1). The release has been investigated as a function of pH to mimic the different physiological environment of healthy tissues (including blood) and tumors. The in vitro cytotoxicity of the releasates from the inorganic matrices has also been investigated.

Materials and Methods

Commercial reagent grade chemicals and solvents were used as received without further purification. *Cis*-1,4-diaminocyclohexane (*cis*-1,4-DACH) was purchased from TCI-Europe. 1,l-Cyclobutanedicarboxylic acid (CBDCA) was purchased from Sigma (Milan). *Cis*-[$PtCl_2(dmso)_2$] (dmso = dimethylsulfoxide) was prepared from an aqueous solution of K_2PtCl_4 and DMSO.[36] Electrospray ionisation mass spectrometry (ESI-MS) was performed with an electrospray interface and an ion trap mass spectrometer (1100 Series LC/MSD Trap system Agilent, Palo Alto, CA).

Elemental analyses were carried out with an Eurovector EA 3000 CHN instrument. ^{1}H-NMR spectra were recorded on a Bruker Avance DPX 300 MHz. ^{1}H chemical shifts were referenced using the internal residual peak of the solvent (DMSO-d_6: 2.50 ppm, D_2O = 4.80 ppm for ^{1}H).

*Synthesis of [Pt(CBDCA)(cis-1,4-DACH)] (compound **2**)*

View Article Online
DOI: 10.1039/C6DT01976E

[Pt(CBDCA)(*cis*-1,4-DACH)] was prepared following the procedure already reported in the literature with slight modifications.[37] CBDCA (944.13 mg, 6.55 mmol) was dissolved in water (270 mL) and neutralized with Ag_2O (1.52 g, 6.55 mmol). After stirring in the dark at room temperature for 20 min, the dicarboxylate solution was treated with c*is*-[$PtCl_2(dmso)_2$] (2.77 g, 6.55 mmol) and the resulting suspension kept under stirring for 10 min at 70 °C and then for 24 h at room temperature in the dark. The suspension was filtered (to separate the AgCl precipitate) and the resulting solution was concentrated to 20 mL under reduced pressure. The solution was then kept at 70 °C for 10 min and then allowed to cool down to room temperature and, successively, kept at 4 °C overnight, meanwhile a white crystalline solid of *cis*-[Pt(CBDCA)$(dmso)_2$] precipitated from the solution. The solid was isolated by filtration of the mother liquor, washed with cold water, and dried in vacuo (2.91 g, 5.89 mmol, yield = 90%). *Anal.* Calculated for [Pt(CBDCA)$(dmso)_2$] ($C_{10}H_{18}O_6S_2Pt$): C, 24.34; H, 3.68%. Found: C, 24.40, H, 3.88%. ^{1}H-NMR (ppm, D_2O): 3.58 (s, 3H), 2.80 (t, $^3J_{H\text{-}H}$ = 7.90 Hz, 4H), 1.94 (quintet, $^3J_{H\text{-}H}$ = 7.90 Hz, 2H). ESI-MS, *m/z* 516 $[M+Na]^+$.

C*is*-[Pt(CBDCA)$(dmso)_2$] (2.91 g, 5.89 mmol) was dissolved in water (140 mL) and treated with a solution of *cis*-1,4-DACH (694 μL, 5.89 mmol) in H_2O (22 mL). The resulting water solution was kept under stirring at 90 °C for 1.5 h. The solution was filtered while hot and then allowed to cool to room temperature. After concentration to a small volume (5 mL) under reduced pressure, the solution was kept at 4 °C overnight. The off-white precipitate was recovered by filtration of the mother liquor, washed with 3 mL ice-cold water and dried under vacuum. It proved to be [Pt(CBDCA)(*cis*-1,4-DACH)] (1.06 g, 2.35 mmol; yield = 40%). *Anal. Calc.* for [Pt(CBDCA)(*cis*-1,4-DACH)]·H_2O ($C_{12}H_{22}O_5N_2Pt$): C, 30.70; H, 4.72; N, 5.97%. *Found*: C, 30.33; H, 4.78; N, 5.86%. ^{1}H-NMR (ppm, D_2O): 3.16 (pseudotriplet, $^3J_{Pt\text{-}H}$ = 100.83 Hz, 2H), 2.89 (t, $^3J_{H\text{-}H}$ = 7.90 Hz, 4H), 1.90 (q, $^3J_{H\text{-}H}$ = 7.90 Hz, 2H), 1.76 (s, 8H). ESI-MS, *m/z* 450 $[M-H]^-$.

View Article Online
DOI: 10.1039/C6DT01976E

*Synthesis of [$PtCl_2$(cis-1,4-DACH)] (kiteplatin, compound **1**)*

Kiteplatin was prepared following the procedure already reported in the literature with slight modifications.[36] [Pt(CBDCA)(*cis*-1,4-DACH)] (1.06 g, 2.35 mmol) was suspended in 95 mL of HCl 1.2 M and stirred for two days at room temperature in the dark. The obtained yellow suspension was taken to dryness by evaporation of the solvent under reduced pressure and the yellow residue was washed with 6 mL of ice-cold water and dried under vacuum. The obtained yellow crystalline product proved to be [$PtCl_2$(*cis*-1,4-DACH)] (0.733 g, 1.93 mmol; yield = 82%). *Anal. Calc.* for [$PtCl_2$(*cis*-1,4-DACH)] ($C_6H_{14}Cl_2N_2Pt$): C, 18.96; H, 3.71; N, 7.37%. *Found*: C, 18.85, H, 3.72, N, 7.29%. ^{1}H-NMR (ppm, DMSO-d_6): 4.90 (s, $^2J_{Pt\text{-}H}$ = 70.00 Hz, 4H) 2.95 (pseudotriplet, $^3J_{Pt\text{-}H}$ = 90.10 Hz, 2H), 1.73-1.66 (br, 4H), 1.48-1.43 (br, 4H). ESI-MS, *m/z* 402 $[M+Na]^+$.

Synthesis of HA nanocrystals

HA nanocrystals were prepared from an aqueous suspension of $Ca(OH)_2$ (1.35 M, 1 L) and $CaCO_3$ (0.1 M, 50 mL) by slow addition of aqueous H_3PO_4 (1.26 M, 600 mL) at room temperature under stirring. The reaction mixture was kept under stirring for 24 hours at room temperature and the resulting homogeneous suspension of HA nanocrystals was used directly to load the compounds under investigation without any further pre-treatment.

Morphological characterization

Transmission electron microscopy (TEM) investigations were carried out using a Philips CM 100 instrument (80 kV). The powdered samples were ultrasonically dispersed in ultrapure water and then

View Article Online
DOI: 10.1039/C6DT01976E

a few droplets of the slurry deposited on holey-carbon foils supported on conventional copper microgrids.

Scanning electronic microscopy (SEM) investigations were carried out using a ZEISS EVO MA 10 instrument with EDX Probe for microanalysis.

Before the analysis, the sample was fixed with apposite glue on the aluminium stub and successfully coated with gold to increase the conductivity of the sample.

FT-IR Analysis

Infrared spectra were recorded on a Nicolet 380 FT-IR spectrometer (Thermo Scientific, Baltimore, MD, USA) equipped with a commercial attenuated total reflectance accessory. The FT-IR spectra were recorded from 4,000 to 400 cm^{-1} at 2 cm^{-1} resolution using an IFS 66v/S spectrometer (Bruker Corporation, Karlsruhe, Germany) and KBr pellets. Spectra were collected by averaging 256 scans at 4 cm^{-1} resolution.

Structural analysis

X-ray powder patterns were collected using an Analytical X'Pert Pro equipped with X'Celerator detector powder diffractometer using Cu Kα radiation generated at 40 kV and 40 mA. The instrument was configured with a 1° divergence and 0.2 mm receiving slits.[38]

The samples were prepared using the front loading of standard aluminium sample holders which are 1 mm deep, 20 mm high and 15 mm wide. The degree of crystallinity was evaluated according to the formula:

$$\text{crystallinity} = (X/Y)\ 100$$

where X = net area of diffracted peaks, and Y = net area of diffracted peaks + background area.

View Article Online
DOI: 10.1039/C6DT01976E

The crystal domain size along the c direction was calculated applying Scherrer's formula:

$$L_{(002)} = \frac{0.94\lambda}{\left[\cos\theta(\sqrt{\Delta r^2 - \Delta_0{}^2})\right]}$$

where θ is the diffraction angle for plane (002), Δr and Δ_0 the widths in radiants of reflection (002) at half height for the synthesized and the reference HA materials, respectively, and λ=1.5405 Å.[39]

Determination of specific surface area

Measurements were performed using a Sorpty 1750 instrument (Carlo Erba) using N_2 absorption at 77 K and the well-known Brunauer, Emmett, and Teller procedure[40]

Platinum determination

The content of platinum loaded onto HA biomimetic nanocrystals was determined by ICP measurements with an HORIBA JOBIN YVON ULTIMA 2 ICP-AES instrument. Aliquots of the sample were dissolved in 10 mL concentrated nitric acid.

Adsorption and release kinetics of platinum complexes from HA nanoparticles.

An aliquot (1.5 mL) of a solution of the platinum complex under investigation (1 mg/mL) was added to 10 mL of a homogeneous HA suspension.

The HA suspension was maintained in a bascule bath at 37 °C under stirring for 24 hours. At scheduled times, aliquots (1 mL) of the supernatant (that was well separated from the solid phase by 4 min of centrifugation at 8000 rpm) were taken off and the platinum content was determined by ICP measurements.

View Article Online
DOI: 10.1039/C6DT01976E

In the release studies, an aliquot of Pt-loaded HA nanoparticles was suspended in physiological-like solution having different pH values (5.0 and 5.5) in order to mimic the environment surrounding a tumor mass. At scheduled times, aliquots (1 mL) of the supernatant (that was well separated from the solid phase by 4 min of centrifugation at 8000 rpm) were taken off and the amount of platinum in the solution determined by ICP-AES measurements.

Experiments with cultured human cells.

The Pt(II) complexes kiteplatin (**1**) and [Pt(CBDCA)(*cis*-1,4-DACH)] (**2**) used in cell experiments were dissolved in 0.9% NaCl solution just before use.

*Preparation of releasates from HA nanocrystals loaded with **1** and **2**.*

For the release experiments, two cell culture media (Nutrient Mixture F-12 Ham and McCoy's) at physiological pH (7.4) and at acidic pH 5.0 or 5.5 (the latter two obtained by addition of citrate buffer 0.1M) were used. Subsequently, 10 mg of unloaded HA, **1**-loaded HA or **2**-loaded HA were suspended in the culture media and, after 15 s of treatment in a vortex apparatus, the suspensions were maintained in a shaking bath at 37 °C. At different time points (0, 5, 30, 60, 120, 240 and 360 min), aliquots of the supernatant were collected. Before proceeding with the cell culture treatments, the pH of the releasates was adjusted to the value of 7.4 to avoid cytotoxicity stemming from acidic pH. For each sample, the amount of platinum released from the HA nanocrystals was quantified by Graphite Furnace Atomic Absorption Spectrometry (GF-AAS) by using a Varian AA Duo graphite furnace atomic absorption spectrometer (Varian, Palo Alto, CA, USA) at 324.7 nm. The calibration curve was obtained using known concentrations of standard solutions purchased from Sigma Chemical Co.

View Article Online
DOI: 10.1039/C6DT01976E

Cell cultures

Human colon (LoVo) and lung (A549) carcinoma cell lines were obtained from American Type Culture Collection (ATCC, Rockville, MD). The human osteosarcoma cell line U2OS and its cisplatin resistant subline, U2OS/Pt cells, were kindly provided by Prof. F. Zunino (Istituto Nazionale per lo Studio e la Cura dei Tumori, Milan, Italy). Cell lines were maintained in the logarithmic phase at 37 °C in a 5% carbon dioxide atmosphere using the following culture media containing 10% fetal calf serum (Euroclone, Milan, Italy), antibiotics (50 units/mL penicillin and 50 μg/mL streptomycin) and 2 mM L-glutamine: (i) McCoy's (Euroclone, Milan, Italy) medium, supplemented with 0.1% gentamicin for U2OS and U2OS/Pt cells; (ii) Nutrient Mixture F-12 Ham (Sigma Chemical Co.) for A549 and LoVo cells.

Cytotoxicity assays

The growth inhibitory effect toward tumor cells was evaluated by means of the MTT assay. Briefly, (5 - 8) x 10^3 cells/well, depending upon the growth characteristics of the cell line, were seeded in 96-well microplates in growth medium (100 μL). After 24 h, the medium was removed and replaced with fresh media containing the compound to be investigated at the appropriate concentration. Triplicate cultures were established for each treatment. After 72 h, each well was treated with 10 μL of a 5 mg/mL MTT saline solution and, following 5 h of incubation, 100 μL of a sodium dodecylsulfate (SDS) solution in 0.01 M HCl were added. After an overnight incubation, the cell growth inhibition was determined by measuring the absorbance of each well at 570 nm using a Bio-Rad 680 microplate reader. The mean absorbance for each drug dose was expressed as a percentage of the absorbance of the control untreated well and plotted *vs* the drug concentration. Data were fitted to a dose–response curve and IC_{50} values, the drug concentrations that decrease the mean absorbance at 570 nm to 50% of those in the untreated,

View Article Online
DOI: 10.1039/C6DT01976E

control wells, were calculated with the four-parameter logistic model (4PL). The final value is the mean ± S.D. of at least three independent experiments performed in triplicate.

Results and discussion

Synthesis of the Pt complexes

Compound **2** is a kiteplatin analog containing the 1,1-cyclobutanedicarboxylate leaving ligand and may be considered related to kiteplatin as carboplatin is related to cisplatin. The synthesis of kiteplatin was modified with respect to that previously reported in the literature by using a dilute solution of HCl to perform substitution of CBDCA by two chlorido ligands. The use of dilute HCl allowed to increase the yield of the reaction (+ 16%) by reducing the amount of the tetrachlorido Pt(IV)-derivative typically formed as side product in the published procedure where concentrated HCl was used. The spectroscopic and spectrometric characterization of the Pt complexes was consistent with literature data.

Biomimetic HA nanocrystals

The synthesized biomimetic hydroxyapatite nanocrystals had composition, structure, morphology, dimension, surface area, and bio-reactivity very close to that of bone inorganic nanocrystals.

The powder X-ray diffraction pattern of the synthesized nanocrystals (Fig. 1A) exhibits not-well defined diffraction maxima that indicate a relatively low degree of crystallinity, which can be estimated to be about 30-32% according to the calculation method described by Sherrer's formula (see Experimental Section). This value is close to that of about 28% determined by the X-ray diffraction pattern of natural, deproteinated bone nanocrystals (Fig. 1B).

View Article Online
DOI: 10.1039/C6DT01976E

The diffraction maxima of the powder X-ray diffraction patterns of the biomimetic HA nanocrystals are characteristic of hydroxyapatite single phase (JCPDS 01-089-6439).

The lamellar morphology of these nanocrystals mimics bone HA. In Fig. 2A is reported the transmission electron microscopy (TEM) image of the synthetized HA nanocrystals. The scanning electron microscopy (SEM) image reported in Fig. 2B shows how the biomimetic HA nanocrystals spontaneously aggregate in micrometric clusters. The EDX analysis (Fig. 3) indicates a Ca/P ratio for the synthetized biomimetic hydroxyapatite nanocrystals very close to that of natural bone hydroxyapatite crystals (ratio close to 1.5).

The FTIR pattern of the synthetized HA nanocrystals is reported in Figure 4 where it is possible to observe the adsorption bands of the phosphate group at 1033 and 1097 cm^{-1} and the characteristic adsorption bands of CO_3^{2-} at 880 cm^{-1}. The amount of CO_3^{2-} is about 5% of the total, resembling the amount of carbonate (4-8%) present in bone nanocrystals.

Synthetized HA nanocrystals exhibit a high bioactivity, due to the large surface area (about 120 m^2/g), and a surface calcium deficiency as in bone HA nanocrystals. At pH 7.4 synthetized HA nanocrystals exhibit a negative electrostatic surface potential (zeta potential of - 20.5±1.5 mV) that would inhibit the occurrence of protein–protein interactions.

*Adsorption of **1** and **2** on HA nanocrystals*

The adsorption experiments were performed at 37 °C in an aqueous medium and monitored for a period of 24 hours. The adsorbed amount of platinum was determined by difference between the initial Pt content in the supernatant solution and that found at different time intervals.

Figure 5 shows the adsorption profiles of the two different platinum complexes on HA nanocrystals in water. This experiment was performed using an innovative procedure, that is

View Article Online
DOI: 10.1039/C6DT01976E

treatment with the Pt complexes of the homogeneous suspension of biomimetic-HA nanocrystals immediately after their synthesis. In this way, the formation of micrometric clusters that partially reduce the reactivity of biomimetic HA nanocrystals is avoided and, as the plots show, an important adsorption of Pt-complex on the surface of the HA nanocrystals takes place in a relatively short time.

Figure 5 also shows that the adsorption kinetics have a similar trend for the two complexes and after 24 h of incubation (in the Figure we report the kinetic only up to 360 min) the percentage of complex adsorbed on the HA nanoparticles, with respect to that initially present in solution, is 89% and 95% for **1** and **2**, respectively. The comparison between the adsorption profiles of the two platinum complexes clearly indicates that the loading of the complexes on the HA nanocrystals most likely occurs by chemical-adsorption of the compounds on the surface of the nanocrystals.

*Release of **1** and **2** from Pt-loaded HA nanocrystals*

For the drug release studies, buffer solutions of different acidity (pH 5.0 or 5.5) were used. The low pH values mimic those typically present in cancer tissues. The release experiments were performed at 37 °C and monitored for a period of 24 hours (in Figure 6 we report the kinetic only up to 360 min). The platinum released from HA (M) was determined by ICP analysis of the supernatant solution as a function of time. The data plotted in Figure 6 are expressed in terms of $M/M_{tot} \times 100$ where M_{tot} corresponds to the amount of complex initially bound to the HA nanocrystals.

Complex **1** exhibits a markedly faster release rate and a greater released amount with respect to complex **2** both at pH 5.0 and 5.5. Being the biomimetic HA nanocrystals more soluble at lower pH, pH 5 probably favors the dissolution of the nanocrystals and, as a consequence, also the release

View Article Online
DOI: 10.1039/C6DT01976E

of the Pt complexes chemisorbed on the HA surface. Remarkably, the amounts of complex released from HA are 2.5 and 1.5 times greater at pH 5.0 compared to pH 5.5 for complexes **1** and **2**, respectively. Although in both cases we observed an initial burst in the release of the Pt compound followed by a constant and sustained release, the trend observed is opposite to the adsorption kinetics, with kiteplatin (**1**) being less adsorbed and more released than **2**.

In order to test if the releasates from the Pt-loaded HA nanocrystals are endowed with cytotoxic activity, the Pt-loaded HA nanocrystals were allowed to release their platinum content into cell culture media (McCoy's and Nutrient Mixture F-12 Ham) conditioned at physiological pH (7.4) and at acidic pH (5.0 and 5.5). The platinum content in cell culture media incubated with unloaded HA, **1**-loaded HA or **2**-loaded HA was assessed by means of GF-ASS analyses (Figure 7).

Both **1**-loaded and **2**-loaded HA nanocrystals release platinum in the cell culture media in time- and pH-dependent manners. At physiological pH both **1**-loaded and **2**-loaded HA release a very scarce amount of platinum, however, at acidic pH, the release of platinum is far greater for **1**-loaded HA (with a maximum release achieved at pH 5.0) than for **2**-loaded HA for which the release of platinum remains rather low, even at pH 5.0. Interestingly, the trend was similar for McCoy's and for Nutrient Mixture F-12 Ham cell culture media. It was confirmed that a lower pH favors the dissolution of the nanocrystals and, as a consequence, also the release of the Pt complexes chemisorbed on the HA surface.

Cell grow inhibitory effect of releasates

The releasates at pH 5.5 and 5.0 from the HA nanocrystals loaded with the Pt complexes were subsequently tested for their cytotoxic potential towards human colon (LoVo) and lung (A549) cancer

View Article Online
DOI: 10.1039/C6DT01976E

cells as well as against human osteosarcoma cells sensitive (U2OS) and resistant (U2OS/Pt) to cisplatin. The latter pair of cell lines was selected since synthetic biomimetic HA nanocrystals are specifically designed to act as prodrugs in the local treatment of bone tumors. In U2OS/Pt cells cisplatin resistance is associated with reduced drug uptake, reduced formation of DNA lesions, defect in the DNA mismatch repair, and upregulation of β-DNA polymerase.[41] The cell viability results (MTT test after 72 h of exposure time) are depicted in Figure 8. The releasates from unloaded HA nanocrystals prove to be non-effective against all tested cell lines (data not shown). On the contrary, the releasate from **1**-loaded HA shows a good in vitro antiproliferative effect against all tested cell lines. The cytotoxic potential increases in a time-dependent manner, with releasates at 360 min being the most effective in decreasing cancer cell viability. Taken together, cytotoxicity results and platinum quantification data strongly confirm that the cytotoxicity of the releasates strictly depends upon the platinum content which, in turn, is modulated by the pH of the cell culture media.

Our results clearly show that releasates of complex **1** are extremely effective in decreasing cell viability, pointing to kiteplatin as the most effective platinum(II) DACH derivative. Interestingly, loaded HA nanoparticles are similarly effective against osteosarcoma sensitive and resistant cells, thus attesting the ability of the compounds to overcome cisplatin resistance. It was rather disappointing the scarce effectiveness of compound **2,** probably due to its very low release from the HA nanovectors. However, this compound should be tested in vivo for which the time scale is much longer than for in vitro tests on cell cultures.

Conclusion

HA nanoparticles are good delivery devices that we have recently developed for the local treatment of bone tumors by loading Pt-bisphosphonate complexes. HA nanoparticles of suitable dimensions could

View Article Online
DOI: 10.1039/C6DT01976E

also be administered by intravenous injection and could accumulate at the tumor site via the EPR effect. The acidic environment of tumor tissues may favor the dissolution of HA and the release of the Pt complexes. In this work we have exploited the adsorption of Pt complexes **1** and **2** on HA nanoparticles. Complex **1**, in particular, has a broad spectrum of activity against tumors. The two Pt(*cis*-1,4-DACH) complexes have been loaded onto the HA nanoparticles soon after their preparation as water suspension. In this way, the lyophilization step has been avoided and with it the possibility of formation of micrometric aggregates of nanoparticles that results in a decrease of drug adsorption on the nanoparticles surface. The adsorption of the complexes was found to be rather fast and the amount of complex loaded very high in both cases with that of **2** slightly greater than that of **1**.

An opposite trend (**1**>**2**) was observed for the release kinetics performed at physiological pH (7.4) and at acidic pH (5.0 and 5.5) to simulate the conditions that are usually observed in the tissues surrounding a tumor mass. The drug release from HA nanoparticles was pH-sensitive. For **1** the release was far greater at acidic pH than at pH 7.4 and, remarkably, a quite big difference was observed between pH 5.5 and pH 5.0. In the case of compound **2** the release remained low even at pH 5.0.

The drug releasates were tested against some selected human cells derived from solid tumors, also including a cisplatin resistant phenotype. Releasates from **1**-loaded HA nanocrystals resulted to be the most cytotoxic against all tested cell lines, being also able to overcome cisplatin resistance.

As the pH in tumor tissues is far more acidic (pH = 5–6) than in the physiological environment (pH = 7.4), our results suggest that the unique characteristics of HA nanoparticles can be exploited for the development of tumor-targeting pH-sensitive nanoparticles.

These preliminary results are of foremost importance since they suggest the potential of kiteplatin-loaded HA nanocrystals as bone-specific drug delivery devices to be used for the treatment of bone tumors upon local implantation. Moreover, HA nanoparticles having suitable dimensions could be

View Article Online
DOI: 10.1039/C6DT01976E

administered by injection and unlike the blood stream, where the high pH value (7.4) will guarantee the stability of the nanocarrier, at the tumor site the acidic pH will promote activation by dissolution of the nanocarrier and release of the Pt drug.

The in vivo investigation that we have planned to perform will hopefully show a potentiated effect due to the dissolution of the HA nanoparticles at the tumor site and consequent release of the platinum drug in addition to high concentrations of Ca^{2+} and PO_4^{3-} that, as mentioned in the Introduction section, can induce the production of inflammatory cytokines that can contribute to the inhibition of tumor cell proliferation.

Acknowledgments

The authors wish to thank the RBAP114AMK, RINAME Project (funds for selected research topics), the C.I.R.M.S.B. (Interuniversity Consortium for Research on Chemistry of Metals in Biological Systems), Qualifu project, Chemical Center Srl and BioEcoActive s.r.l. The Authors thank Dr. Salvatore Savino (University of Bari) for assistance in the preparation of the platinum compounds.

References

1 S. Pietronave, M. Iafisco, D. Locarno, L. Rimondini, M. Maria Prat, *J. Appl. Biomater. Biomech.*, 2009, **7**, 77-89.

2 N. Roveri, P. Barbara and M. Iafisco, *Expert Opin Drug Deliv.,* 2008, **5**, 861-877.

3 H. Hillaireau and P. Couvreur, *Cell. Mol. Life Sci*., 2009, **66**, 2873-2896.

4 J.H. Adair, M.P. Parette, E.I. Altınoğlu and M. Kester*, ACS Nano*, 2010, **4**, 4967-4970.

5 F.C.M. Driessens, J.W.E. van Dijk and J.M.P.M. Borggreven, *Calcif. Tissue Int*., 1978, **26**, 127-136.

6 M. Vallet-Regí and J.M. Gonzalez-Calbet, *Prog. Solid State Chem.*, 2004, **32**, 1-31.

7 L. Wang, G.H. Nancollas, Z.J. Henneman, E. Klein and S. Weiner, *Biointerphases*, 2006, **1**, 106-111.

8 H. A. Lowenstam and S. Weiner, On Biomineralization, Oxford University Press: USA, 1989.

View Article Online
DOI: 10.1039/C6DT01976E

9 H. Gao, B. Ji, I.L. Jager, E. Arz and P. Fratzl, *Proc. Natl. Acad. Sci. U. S. A.*, 2003, **100**, 5597-5660.

10 H.S. Gupta, J. Seto, W. Wagermaier, P. Zaslansky, P. Boesecke and P. Fratzl, Proc. Natl. Acad. Sci. U. S. A., 2006, **103**, 17743-17746.

11 S. Weiner and L. Addadi, *J. Mater. Chem.*, 1997, **7**, 689-702.

12 T. A. Kuriakose, S. N. Kalkura, M. Palanichamy, D. Arivuoli, K. Dierks, G. Bocellif and C. Betzel, *J. Cryst. Growth*, 2004, **263**,517-523.

13 A.C. Tas, *Biomaterials*, 2000, **21**, 1429-1438.

14 L.W. Suchanek, P. Shuk, K. Byrappa, R.E. Riman, K.S. TenHuisen and V.F. Janas, *Biomaterials*, 2002, **23**, 699-710.

15 A. Ruksudjarit, K. Pengpat, G. Rujijanagul and T. Tunkasiri, *Curr. Appl. Phys.*, 2008, **8**, 270-272.

16 N. Roveri and B. Palazzo, in *Tissue, Cell and Organ Engineering (Nanotechnologies for the Life Sciences)*; ed. C. S. S. R. Kumar, Wiley-VCH: Weinheim, 2006, pp 283–307.

17 M. Iafisco, B. Palazzo, G. Falini, M. Di Foggia, S. Bonora, S. Nicolis, L. Casella and N. Roveri, *Langmuir*, 2008, **24**, 4924-4930.

18 X.M. Liu, H.T. Lee, R.A. Reinhardt, L.A. Marky and D. Wang, J. *Controlled Release*, 2007, **122**, 54.

19 X. Cheng and L. Kuhn, *Int. J. Nanomed.*, 2007, **2**, 667-674.

20 A. Barroug and M. Glimcher, *J. Orthop. Res.*, 2002, **20**, 274-280.

21 T. Xu, N. Zhang, H. L. Nichols, D. Shi and X. Wen, *Mater. Sci. Eng.*, 2007, **27**, 579-594.

22 M. Stigtera, J. Bezemera, K. de Grootb and P. Layrollec, *J. Controlled Release*, 2004, **99**, 127-137.

23 N. Nocerino, A. Fulgione, M. Iannaccone, L. Tomasetta F. Ianniello F. Martora M. Lelli N. Roveri F. Capuano and R. Capparelli, *Int J Nanomedicine*, 2014, **9**, 1175-1184.

24 N. Roveri and M. Iafisco, *Nanotech Sci Appl*., 2010, **3**,107-125.

25 M. Benedetti, F. De Castro, D. Migoni, A. Romano, T. Verri, M. Lelli, N. Roveri and F.P. Fanizzi, *J Inorg Biochem.*, 2016, **157**, 73-79.

26 M. Benedetti, D. Antonucci, F. De Castro, C.R. Girelli, M. Lelli, N. Roveri and F.P. Fanizzi, *J Inorg Biochem.*, 2015,**153**, 279-283.

27 A. Rimola, Y. Sakhno, L. Bertinetti, M. Lelli, G. Martra and P. Ugliengo, *J. Phys. Chem. Lett.*, 2011,**2**, 1390-1394.

28 B. Palazzo, M. Iafisco, M. Laforgia, N. Margiotta, G. Natile, C.L. Bianchi, D. Walsh, S. Mann and N. Roveri, *Adv. Funct Mater.,* 2007, **17**, 2180-2188.

29 M. Iafisco, B. Palazzo, M. Marchetti, N. Margiotta, R. Ostuni, G. Natile, M. Morpurgo, V. Gandin, C. Marzano and N. Roveri, *J. Mater. Chem.,* 2009, 19, 8385-8392.

30 M. Iafisco, B. Palazzo, G. Martra, N. Margiotta, S. Piccinonna, G. Natile, V. Gandin, C. Marzano and N. Roveri, *Nanoscale,* 2012, **4**, 206-217.

View Article Online
DOI: 10.1039/C6DT01976E

31 M. Iafisco and N. Margiotta. *J. Inorg. Biochem.,* 2012, **117**, 237-242.

32 V. Uskokovic and D.P. Uskokovic, *J. Biomed. Mater. Res.*, 2011, **96**, 152-191.

33 S. Dey, M. Das and V.K. Balla. *Mater. Sci. Eng. C.*, 2014, **39**, 336-339.

34 L. Kelland, *Nat. Rev. Cancer*. 2007, **7**, 573–584.

35 N. Margiotta, C. Marzano, V. Gandin, D. Osella, M. Ravera, E. Gabano, J.A. Platts, E. Petruzzella, J.D. Hoeschele and G. Natile, *J. Med. Chem*. 2012, **55**, 7182-7192.

36 Yu. N. Kukushkin, Yu. E. Vyaz'menskii, L.I. Zorina, Yu. L. Pazukhina, *Zh. Neorg. Khim*. 1968, **13**, 1595-1599.

37 R. Ranaldo, N. Margiotta, F.P. Intini, C. Pacifico, G. Natile, *Inorg. Chem.,* 2008, **47**, 2820-2830.

38 B.V. Almelo, X'PERT HIGH SCORE (version 2.0a), PANalytical, The Netherlands, 2004**.**

39 H.P. Klug*,* L.E. Alexander*, X-Ray Diffraction Procedures*, John Wiley and Sons, New York, 1954.

40 S. Brunauer, P.H. Emmett, E. Teller, *J Am Chem Soc*., 1938, **60**: 309–319.

41 S. Mazzega Sbovata, F. Bettio, M. Mozzon, R. Bertani, A. Venzo, F. Benetollo, R.A. Michelin, V. Gandin, C. Marzano, *J Med Chem*., 2007, **50**, 4775-84.

View Article Online
DOI: 10.1039/C6DT01976E

Figure captions

Chart 1. Structures of platinum drugs currently approved by FDA (cisplatin, carboplatin, and oxaliplatin), kiteplatin (**1**), and [Pt(CBDCA)(*cis*-1,4-DACH)] (**2**).

Fig. 1 (A) XRD spectra of biomimetic HA nanocrystals prepared in this work; **(B)** XRD spectra of reference Bone-HA.

Fig. 2 (A) Transmission Electronic Microscopy (TEM) Image of Biomimetic HA nanocrystals with acicular morphology, **(B)** Scanning Electronic Microscopy (SEM) image of spontaneously formed micrometric aggregates of biomimetic HA nanocrystals.

Fig. 3 Elementary analysis performed with EDX probe on biomimetic HA nanocrystals. In evidence the presence of Calcium (Ca) and Phosphorous (P) in the typical ratio Ca/P of biomimetic HA.

Fig. 4 FT-IR Spectra of biomimetic HA nanocrystals. In evidence the characteristic adsorption bands of Hydroxyapatite.

Fig. 5 Kinetic of drugs adsorption (complex **1** and **2**) on biomimetic HA nanocrystals.

Fig. 6 Released Pt percentages from HA nanocrystals loaded with complexes **1** and **2.** Two pH values (5.0 and 5.5) were considered.

Fig. 7 Platinum released from **1**-loaded HA or **2**-loaded HA suspended in cell culture media (F-12 Ham, panel A, and Mc Coy's panel B) at pH 7.4 or acidic pH 5.0 and 5.5. At different time points (0, 5, 30, 60, 120, 240 and 360 min) aliquots of the supernatant were collected and the platinum content in each sample was quantified by means of GF-AAS analysis. Error bars indicate SD.

Fig. 8 Cytotoxicity tests. Cells (5–8×104 mL) were treated for 72 h with cell culture media used to investigate the Pt-release from **1**-loaded HA nanocrystals (A) or **2**-loaded HA nanocrystals (B) at different time points. Cytotoxicity was assessed by MTT test. Data are the means of at least three independent experiments. Error bars indicate SD.

View Article Online
DOI: 10.1039/C6DT01976E

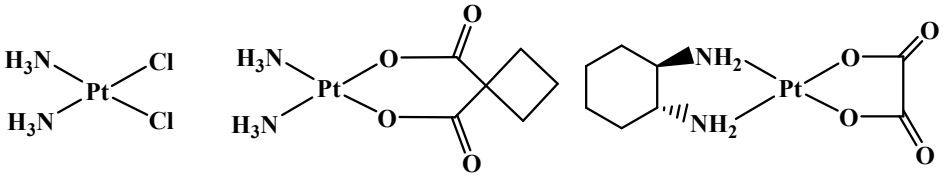

Cisplatin **Carboplatin** **Oxaliplatin**

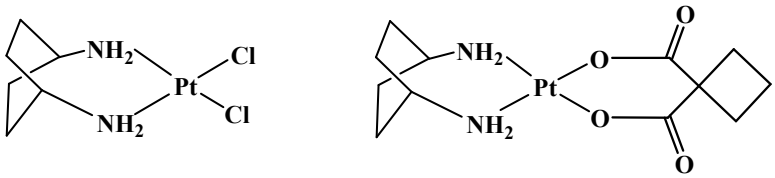

Kiteplatin (1) **[Pt(CBDCA)(*cis*-1,4-DACH)] (2)**

Chart 1

View Article Online
DOI: 10.1039/C6DT01976E

Figure 1

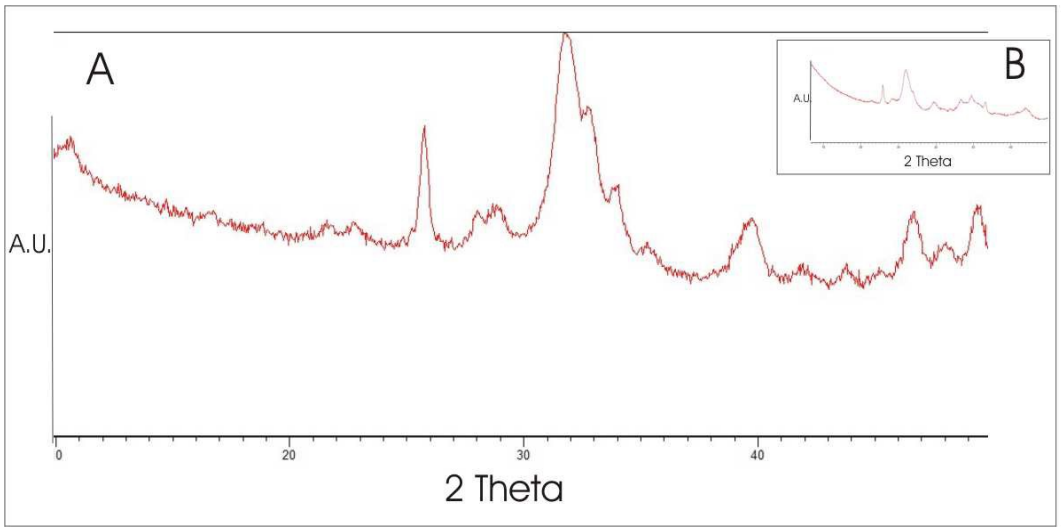

View Article Online
DOI: 10.1039/C6DT01976E

Figure 2

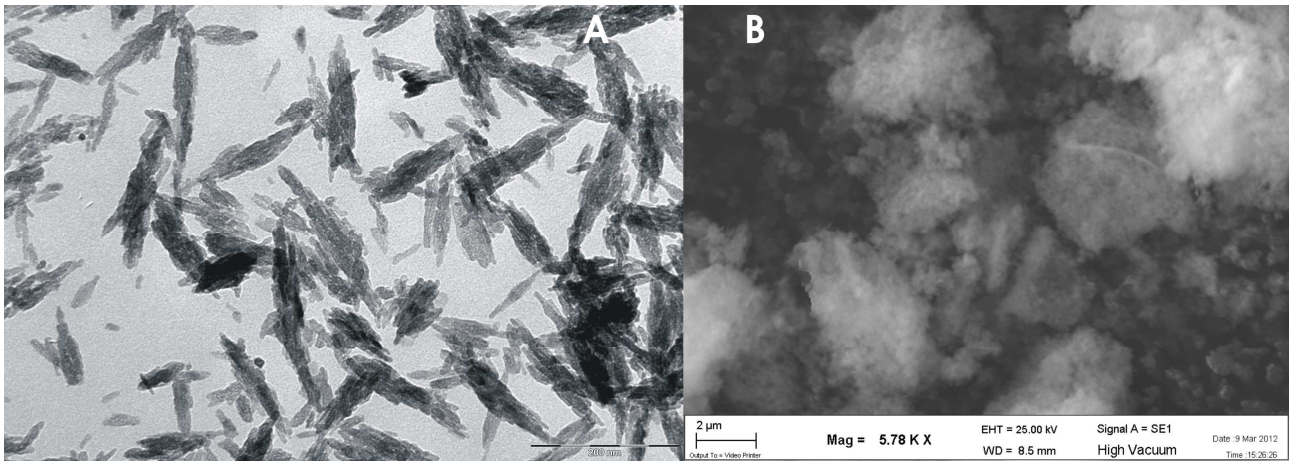

View Article Online
DOI: 10.1039/C6DT01976E

Figure 3

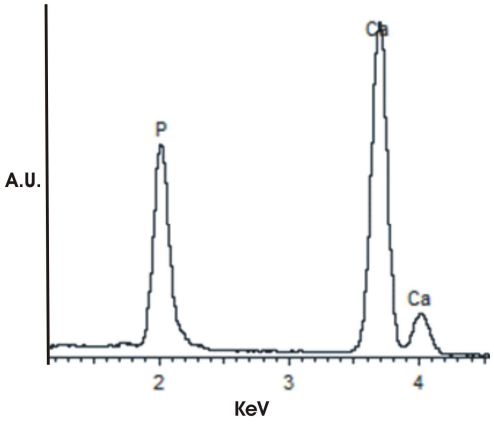

View Article Online
DOI: 10.1039/C6DT01976E

Figure 4

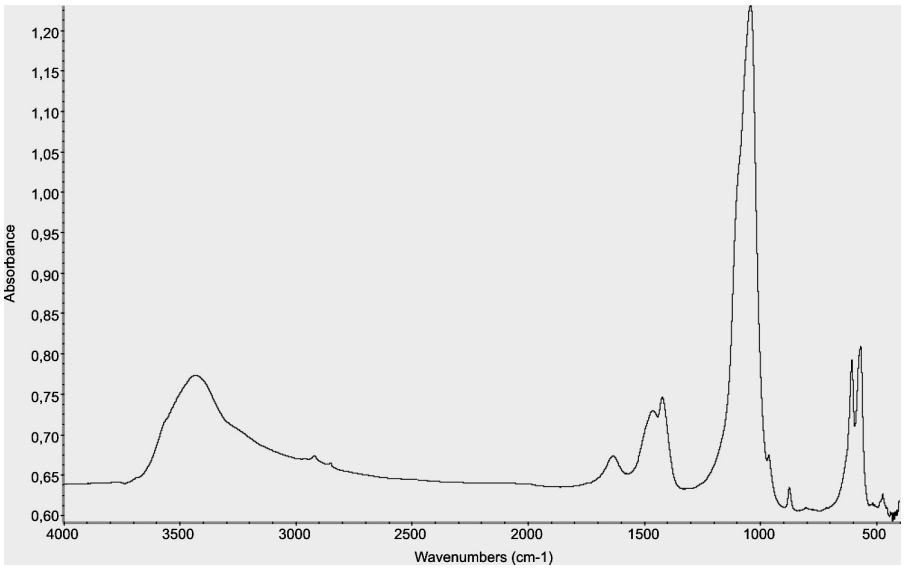

View Article Online
DOI: 10.1039/C6DT01976E

Figure 5

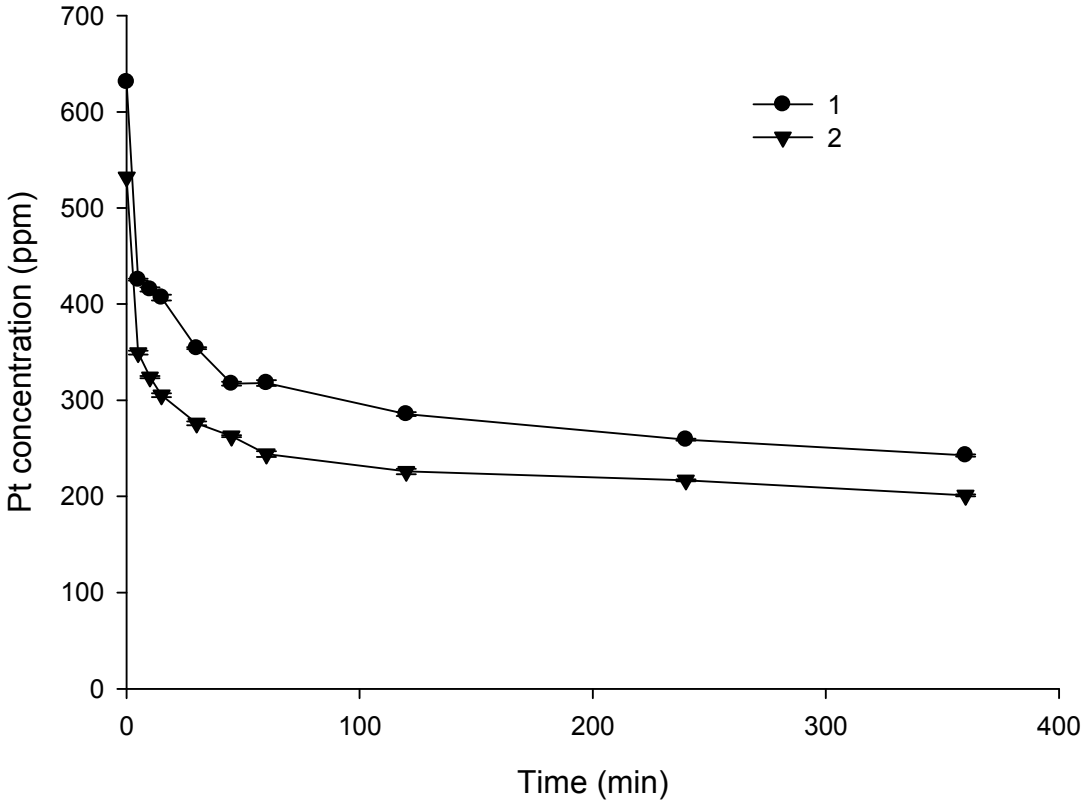

Adsorption of complex **1** and complex **2** onto HA as a function of time.

View Article Online
DOI: 10.1039/C6DT01976E

Figure 6.

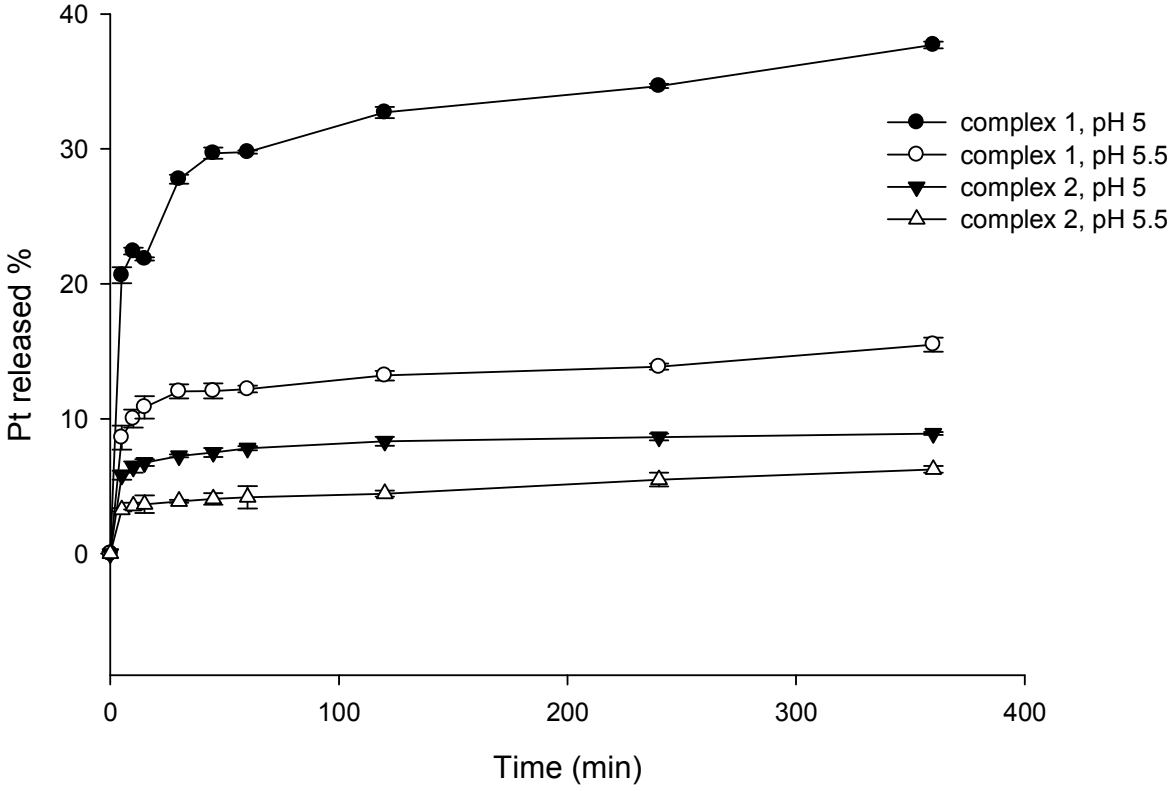

View Article Online
DOI: 10.1039/C6DT01976E

Figure 7

A

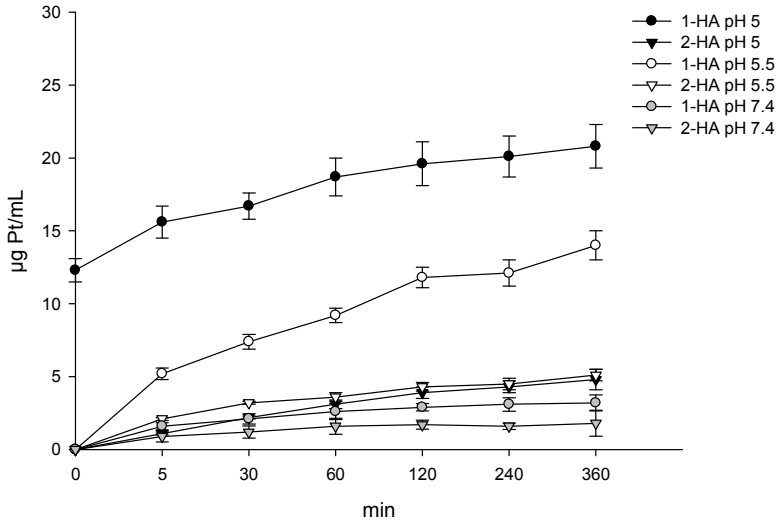

B

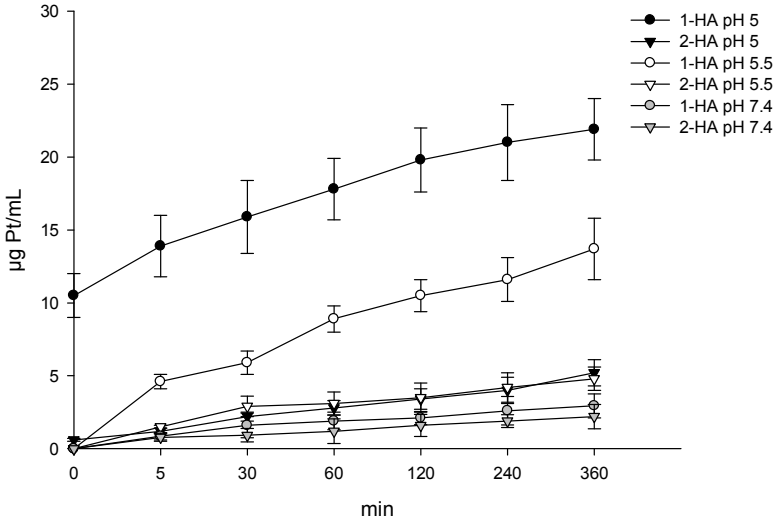

View Article Online
DOI: 10.1039/C6DT01976E

Figure 8.

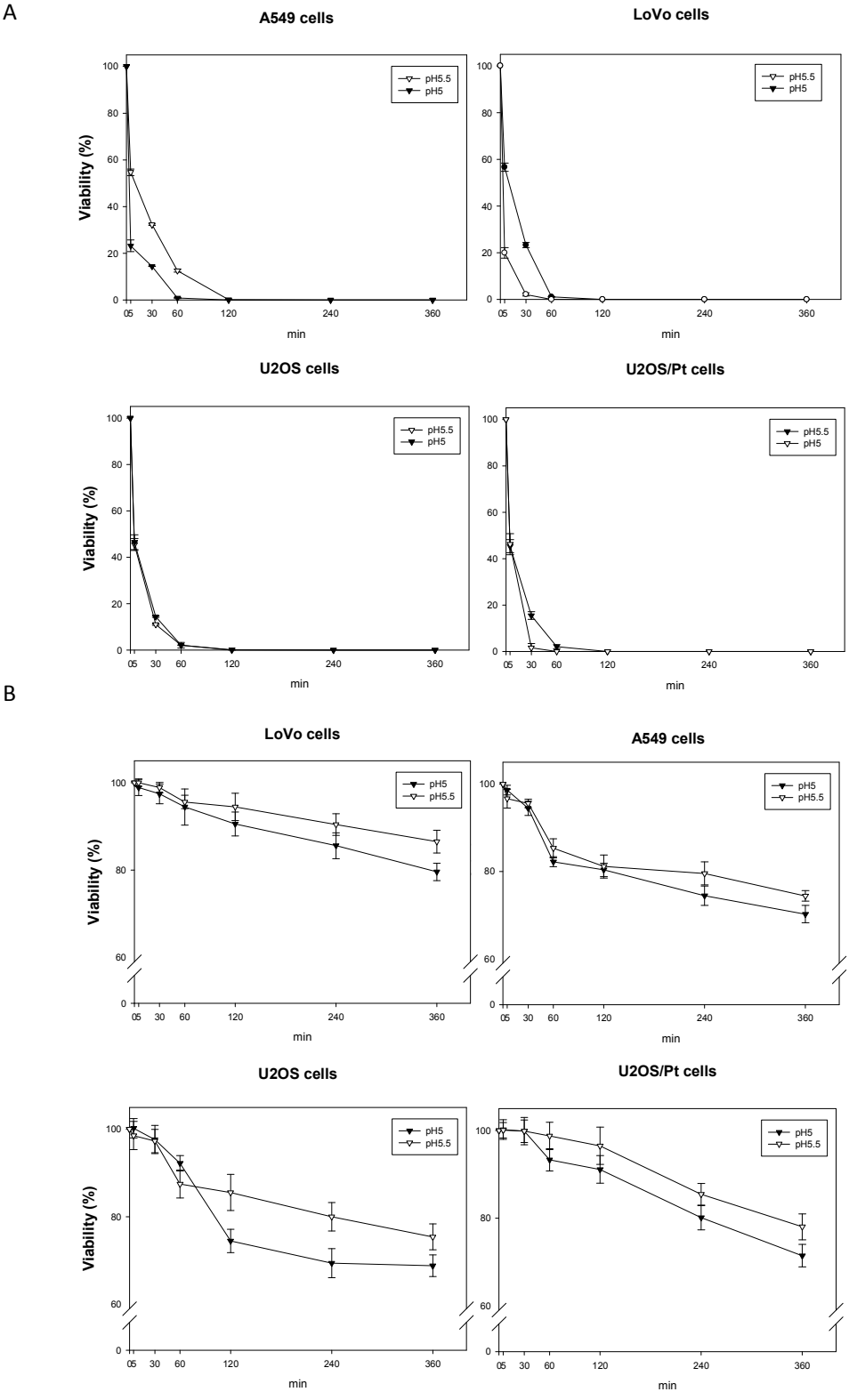

View Article Online
DOI: 10.1039/C6DT01976E

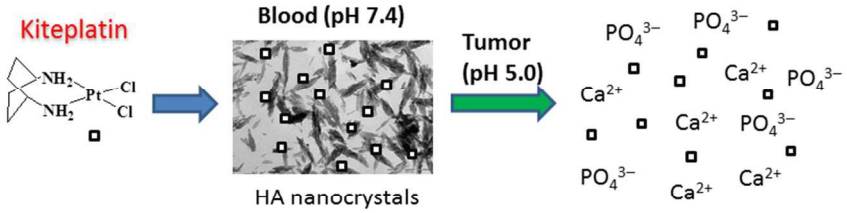

254x190mm (96 x 96 DPI)